Available online at www.sciencedirect.com
ScienceDirect
Trans. Nonferrous Met. Soc. China 26(2016) 1491−1497
Transactions of Nonferrous Metals Society of China
www.tnmsc.cn

Dynamic recrystallization behavior of 7085 aluminum alloy during hot deformation

Dong-feng LI[1,2,3], Duan-zheng ZHANG[1,2], Sheng-dan LIU[1,2,4], Zhao-jun SHAN[1,2], Xin-ming ZHANG[1,2,4], Qin WANG[1,2], Su-qi HAN[1,2]

1. School of Materials Science and Engineering, Central South University, Changsha 410083, China;
2. Key Laboratory of Nonferrous Metal Materials Science and Engineering, Ministry of Education, Central South University, Changsha 410083, China;
3. School of Mechanical Engineering, Hunan Institute of Engineering, Xiangtan 411104, China;
4. Nonferrous Metal Oriented Advanced Structural Materials and Manufacturing Cooperative Innovation Center, Central South University, Changsha 410083, China

Received 29 July 2015; accepted 25 February 2016

Abstract: The dynamic recrystallization behavior of 7085 aluminum alloy during hot compression at various temperatures (573−723 K) and strain rates (0.01−10 s^{-1}) was studied by electron back scattered diffraction (EBSD), electro-probe microanalyzer (EPMA) and transmission electron microscopy (TEM). It is shown that dynamic recovery is the dominant softening mechanism at high Zener−Hollomon (Z) values, and dynamic recrystallization tends to appear at low Z values. Hot compression with ln Z=24.01 (723 K, 0.01 s^{-1}) gives rise to the highest fraction of recrystallization of 10.2%. EBSD results show that the recrystallized grains are present near the original grain boundaries and exhibit similar orientation to the deformed grain. Strain-induced boundary migration is likely the mechanism for dynamic recrystallization. The low density of Al_3Zr dispersoids near grain boundaries can make contribution to strain-induced boundary migration.

Key words: aluminum alloy; Zener−Hollomon parameter; dynamic recrystallization; strain-induced boundary migration; Al_3Zr dispersoids

1 Introduction

Dynamic recrystallization (DRX) often occurs in aluminum and aluminum alloys during hot deformation, and generally there are continuous dynamic recrystallization (CDRX) and discontinuous dynamic recrystallization (DDRX) [1,2]. In most aluminum alloys, DDRX was rarely observed because of its high tendency to recover [3,4]; however, some recent investigations have shown that DDRX may occur in Al−Mg, Al−Cu−Li and Al−Zn−Mg−Cu alloys [5−7]. CDRX was reported to occur at high temperatures and low strain rates [5,8,9], and at severe strain geometric dynamic recrystallization (GDRX) tends to occur [7,8]. It is known that particle-stimulated nucleation (PSN), strain-induced boundary migration (SIBM) or subgrain rotation (SGR) is the possible mechanism of DRX. PSN may lead to DDRX because second phase particles can induce a high gradient dislocation density around them during deformation, which may stimulate recrystallization nucleation and growth [10]. SIBM may occur during DRX as well, and the driving force is the difference in the density of dislocations; grain boundaries (GBs) can bulge into the regions with a high density of dislocations [10]. SGR, which often occurs in the interior of original grains, generally results in CDRX [11].

Recrystallization has great influence on the properties of aluminum alloys. For instance, in Al−Zn−Mg−Cu alloys, which are called aeronautical Al alloys [12], the occurrence of recrystallization can decrease strength, toughness and corrosion resistance and increase quench sensitivity. HAN et al [13] reported that the increase of recrystallization fraction leads to lower strength and fracture toughness of 7050 aluminum alloy. KANNAN and RAJA [14] reported that it is possible to

Foundation item: Project (2012CB619500) supported by the National Basic Research Program of China
Corresponding author: Sheng-dan LIU; Tel/Fax: +86-731-88830265; E-mail: csuliusd@163.com
DOI: 10.1016/S1003-6326(16)64254-1

enhance stress corrosion resistance of Al−Zn−Mg−Cu−Zr alloys by inhibiting recrystallization. LIU et al [15] found that recrystallization results in a larger amount of high angle boundaries and incoherent dispersoids, and consequently increases quench sensitivity of 7055 aluminum alloy. Therefore, it is essential to inhibit recrystallization so as to further improve properties of these alloys. In these aluminum alloys, there are some possible ways to inhibit recrystallization. One is to promote uniform precipitation of fine Al_3M (M=Zr, Sc, etc) dispersoids [16,17], which can hinder the migration of subgrain boundaries and grain boundaries; the second one is to decrease the amount of large second phase particles so as to minimize PSN [18]; the third one is to decrease stored deformation energy, for instance, by elevating temperature slowly during solution heat treatment or by stepped solution heat treating [13,19]. However, during hot deformation, dynamic recrystallization may be triggered due to the increased deformation energy, and this may exert great influence on the static recrystallization during subsequent solution heat treatment. Therefore, it is desirable to have better understanding of the DRX behavior of these alloys, though studies have been done on hot deformation behavior of some Al−Zn−Mg−Cu alloys, such as 7075, 7050 and 7150 alloys [2,20,21].

In this work, dynamic recrystallization behavior of 7085 aluminum alloy was investigated, and this is helpful for controlling recrystallization and obtain combination of high strength and corrosion resistance.

2 Experimental

The material was a 7085 aluminum alloy ingot with chemical composition of Al−7.59Zn−1.65Mg−1.54Cu−0.11Zr (mass fraction, %). The ingot was homogenized at 743 K for 24 h and then cooled in air. Small cylindrical specimens with 10 mm in diameter and 15 mm in height were machined from the homogenized ingot. Uniaxial compression tests were conducted on a Gleeble 3500 thermomechanical simulation unit at temperatures of 573−723 K with strain rates of 0.01−10 s^{-1}. The specimens were heated to the desirable deformation temperature with a heating rate of 3 K/s, held for 2 min and then compressed. All specimens were deformed to a true strain of 0.7 and then quenched in room temperature water immediately to freeze the as-deformed microstructure.

All deformed specimens were sectioned parallel to the compression axis along the centerline for microstructure examination. Electron back scattered diffraction (EBSD) technique was used to examine the microstructure of the specimens so as to obtain information about DRX; this was performed on a ZEISS-EVO18 scanning electron microscope (SEM), and the scanning step size was 1.75 μm and the results were analyzed using HKL Channel 5 software. The distribution of alloying elements in the grains was examined by electro-probe microanalyzer (EPMA). Some specimens were mechanically thinned to a thicknesses of about 80 μm, punched into foils of 3 mm in diameter, electropolished in 30% HNO_3 and 70% CH_3OH solution below −30 °C and then observed on a JEOL−2100F transmission electron microscope (TEM) operated at 200 kV to examine the microstructure.

3 Results and discussion

The true stress−strain curves during hot compression of 7085 aluminum alloy at strain rates of 0.01−10 s^{-1} and at temperatures of 573−723 K are presented in Fig. 1. The peak stress tends to increase with the increase of strain rate or the decrease of temperature, which is similar to previous investigations on Al−Zn−Mg−Cu alloys [2,20,21]. In general, an initial rapid increase in the flow stress can be seen with the increase of strain; however, the shape of the flow curves was changed by strain rate. At low strain rates of 0.1 s^{-1} and 0.01 s^{-1}, the flow stress tends to be constant with the further increase of strain; at 1 s^{-1}, the flow stress increases slightly; at 10 s^{-1}, the flow stress tends to decrease especially at the temperature of 573 K. Moreover, the stress−strain curves are serrated at the rates of 1 s^{-1} and 10 s^{-1}, which may indicate alternate occurrence of dynamic hardening and dynamic softening [5,21]. The fall of flow stress at the highest strain rate of 10 s^{-1} (Fig. 1(a)) shows that dynamic softening and work hardening lose balance, which may be attributed to the adiabatic heating [22].

The softening mechanism may be deduced by microstructure examination. In order to describe the influence of hot deformation parameters on microstructure, a Zener−Hollomon (Z) parameter was used, and therefore the effect of both temperature and strain rate can be taken into consideration [1]. The Z parameter can be expressed as

$$Z = \dot{\varepsilon}\exp\left(\frac{Q}{RT}\right) \tag{1}$$

where $\dot{\varepsilon}$ is strain rate, T is temperature, R is the mole gas constant, Q is the apparent activation energy. Q value was determined to be 172.0 kJ/mol [23], and the value of Z can be calculated under various hot deformation conditions.

Orientation imaging maps of the specimens under various hot deformation conditions are given in Fig. 2. It can be seen that grains are elongated after hot deformation, and Z values have significant effects on the

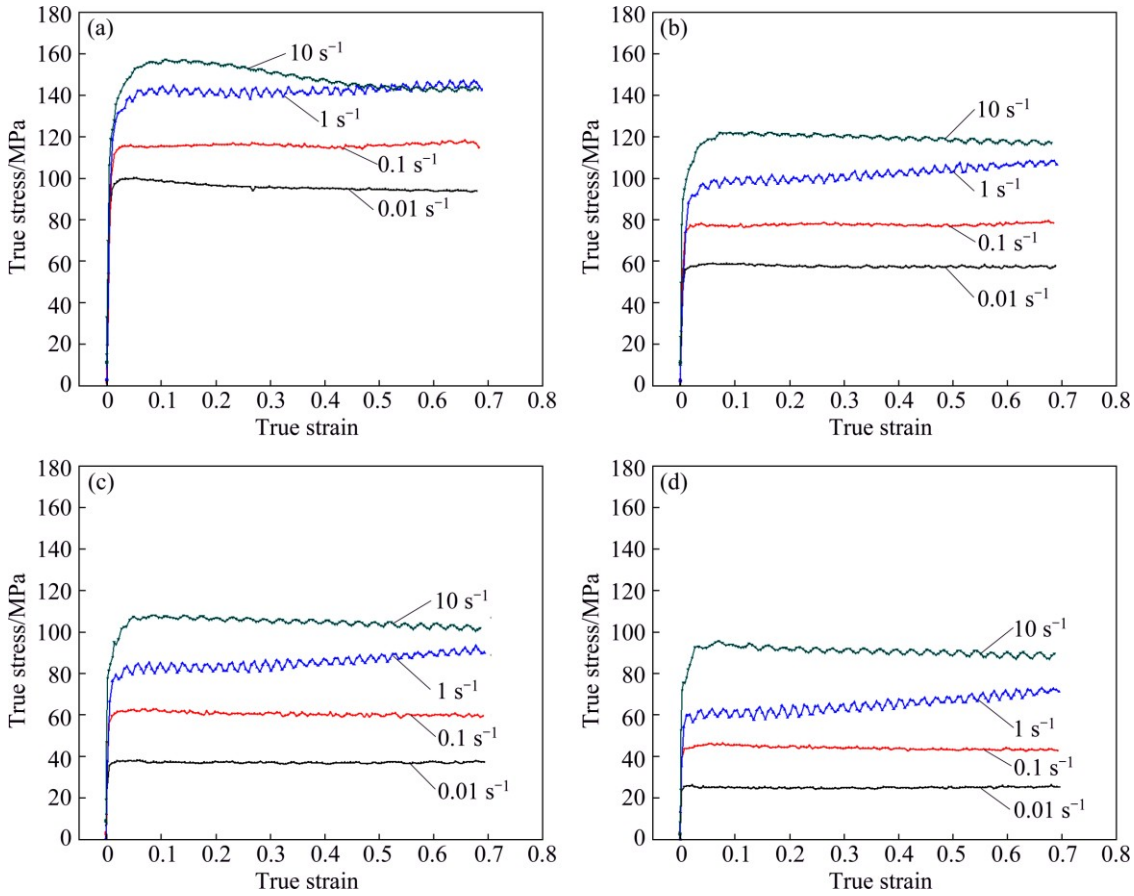

Fig. 1 True stress−strain curves of 7085 aluminum alloy during hot compression: (a) 573 K; (b) 623 K; (c) 673 K; (d) 723 K

microstructure. For high Z values, as shown in Figs. 2(a) and (b), there are many thin black lines in the interior of grains, which may indicate a high density of cells or substructures. With the decrease of Z value to 28.44, the number of cells or substructures decreases significantly, and they tend to locate near original GBs (Fig. 2(c)). For lower Z values, cells and substructures seem to disappear and some subgrains and recrystallized grains may be seen (Figs. 2(d) and (f)). It is likely that for high Z values dynamic recovery (DRV) is the dominant softening mechanism, and for low Z values both DRV and DRX make contribution to softening during deformation. Recrystallized grains tend to be present near the serrated original grain boundaries and at triple GBs junction (Fig. 2(f)); few recrystallized grains can be associated with second phase particles, which may indicate that PSN is not the likely recrystallization mechanism. Moreover, characteristics of GDRX could not be found, and therefore it is reasonable to conclude that GDRX did not occur during deformation. After a careful look in Figs. 2(d) and (f), it can be found that recrystallized grains exhibit similar color as the deformed grain, which may indicate that they have similar orientation. And it is probably that no SGR occurred during hot deformation. Therefore, SIBM is the most likely recrystallization mechanism.

Furthermore, a quantitative analysis was performed to show the effect of Z values on the microstructural characteristics, and the results are given in Fig. 3. From Fig. 3(a), it seems that the fraction of low angle boundaries (LABs) increases slightly and correspondingly that of high angle boundaries (HABs) decreases with the increase of Z values. From Fig. 3(b), the fraction of deformed regions increases rapidly with the increase of Z value from 24.01 to 28.44, and then only slightly at higher Z values; the fractions of substructured and recrystallized regions exhibit an opposite trend. A higher fraction of LABs may indicate a higher fraction of deformed microstructure and substructures; while an increased fraction of HABs indicates the occurrence of DRX. The highest fraction of DRX of about 10.2% was observed at ln Z=24.01 (723 K, 0.01 s^{-1}). In order to have a better understanding of DRX in this alloy, further microstructure examination by TEM and EPMA were carried out, and typical results are shown in Figs. 4 and 5.

Figure 4 shows the TEM bright field images and selected area diffraction patterns of the homogenized and as-deformed specimens. In the homogenized specimen, some coherent or semi-coherent Al_3Zr dispersoids with

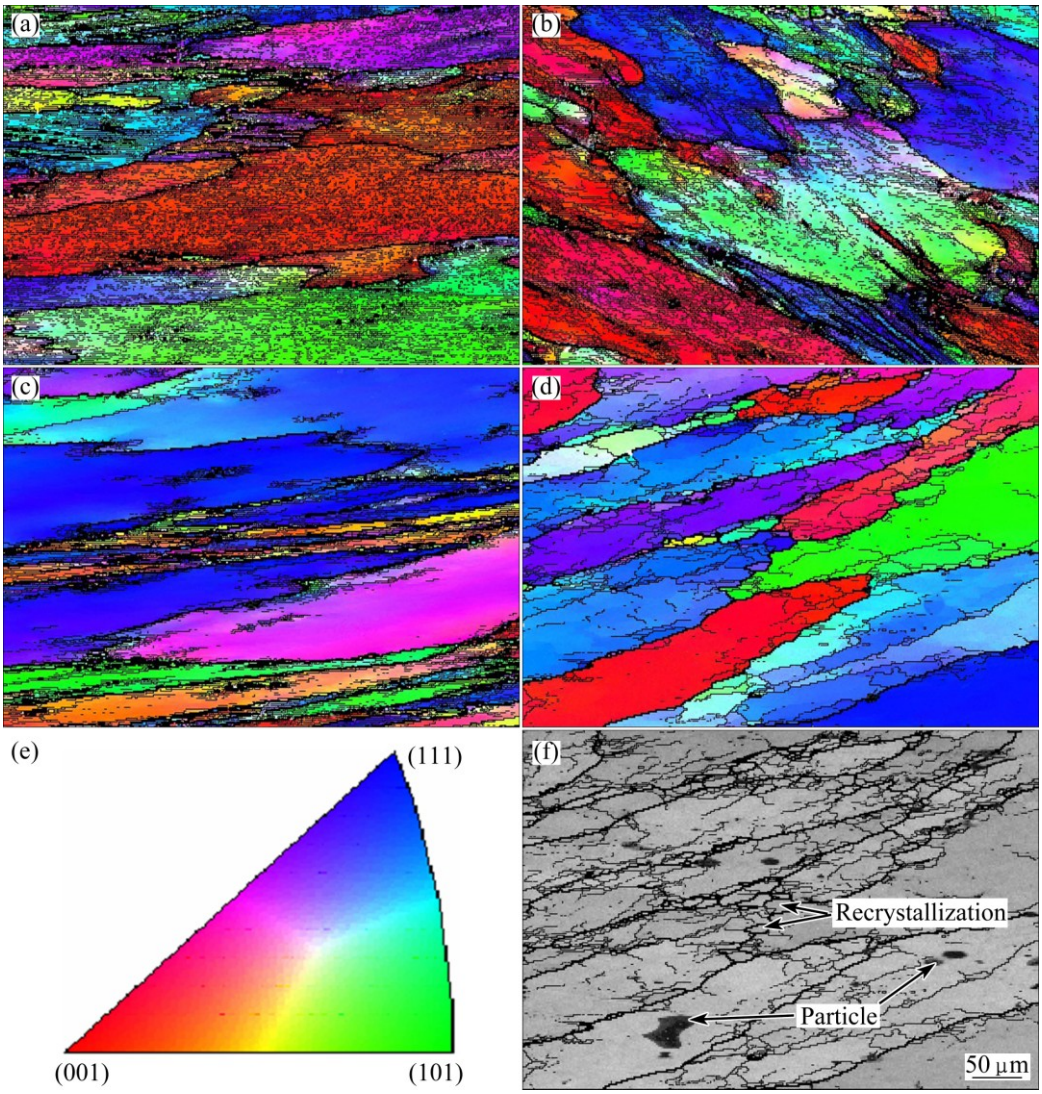

Fig. 2 EBSD imaging maps of specimens deformed under different hot deformation conditions: (a) ln Z=36.10 (623 K, 10 s^{-1}); (b) ln Z=31.5 (723 K, 10 s^{-1}); (c) ln Z=28.44 (673 K, 0.1 s^{-1}); (d, f) ln Z=24.01(723 K, 0.01 s^{-1}); (e) Representation of color code used to identify crystallographic orientations on standard stereographic projection (red: [001]; green: [101]; blue: [111]); (f) Image quality map related to (d)

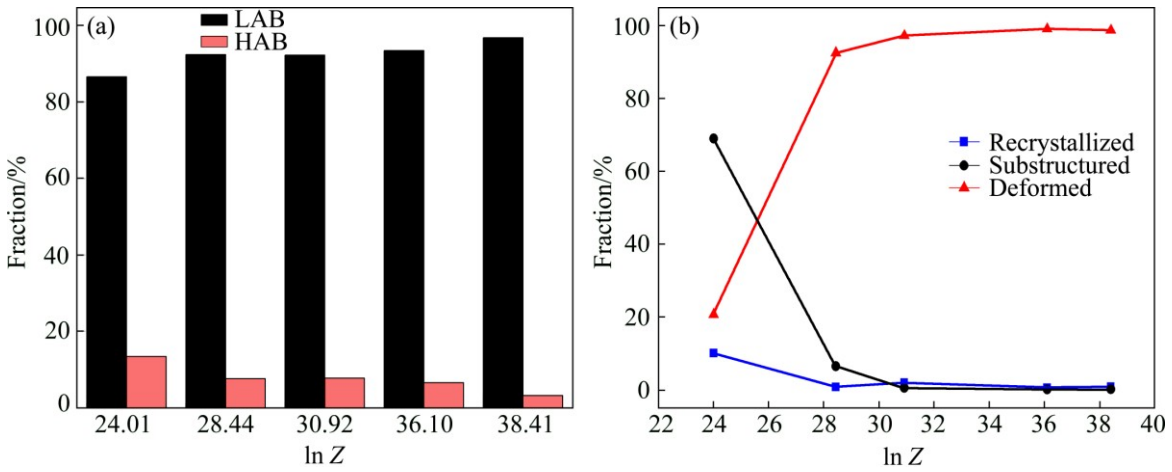

Fig. 3 Effects of Z values on fraction of boundaries (a) and fraction of deformed, substructured and rerystallized microstructures (b)

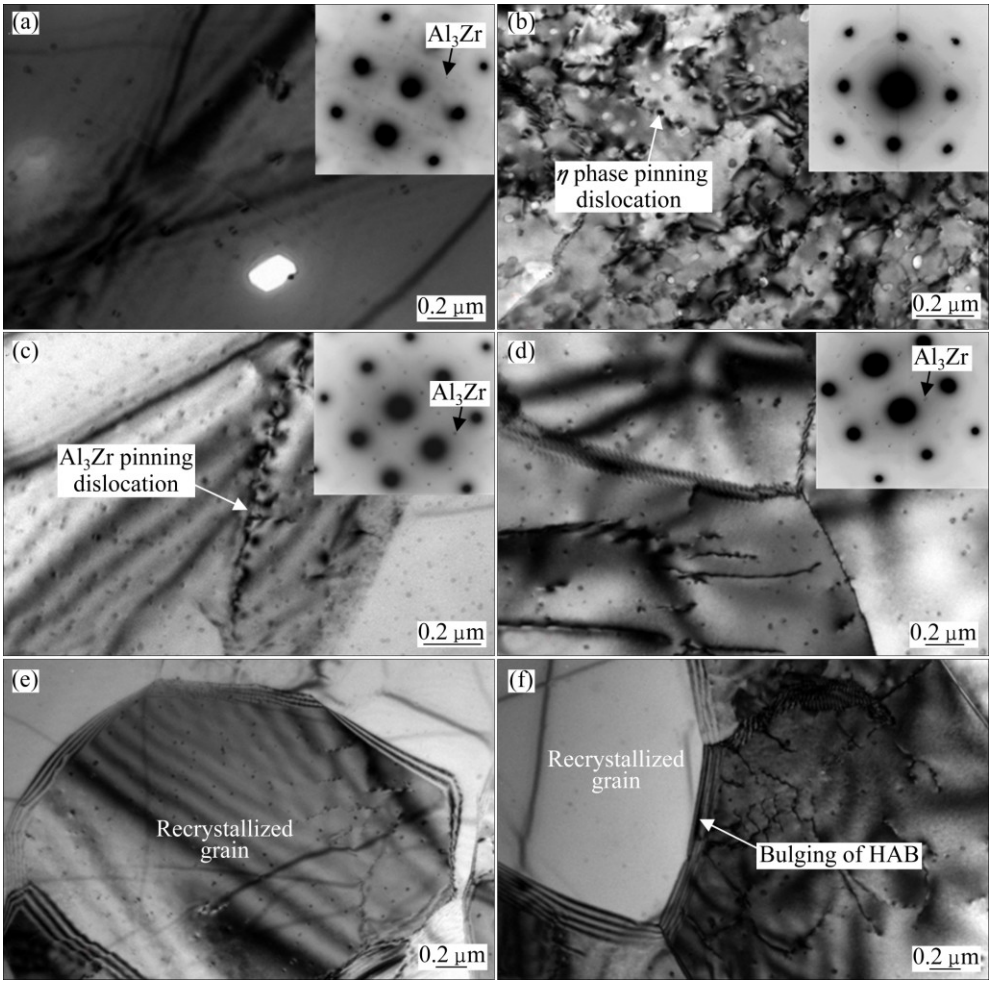

Fig. 4 TEM images of homogenized and as-deformed specimens: (a) Homogenized; (b) ln Z=36.10 (623 K, 10 s^{-1}); (c) ln Z=31.5 (723 K, 10 s^{-1}); (d−f) ln Z=24.01 (723 K, 0.01 s^{-1}), subgrain (d), recrystallized grain (e) and grain boundary (f)

no-contrast lines can be seen in the interior of grains (Fig. 4(a)). These dispersoids can inhibit recrystallization during hot deformation and solution heat treatment [15,18]. At high Z values, for instance, ln Z=36.10, the interaction between dislocations and nanoscale particles can be observed (Fig. 4(b)). Apart from Al_3Zr dispersoids, these nanoscale particles include η phase ($Mg(Zn, Cu)_2$). These dense and fine particles can exert strong pinning effects on dislocation movement. At lower Z values, few nanoscale η phase particles can be identified. It is Al_3Zr dispersoids that pin dislocations and subgrain boundaries (Figs. 4(c) and (d)). During hot deformation at high strain rates, dislocations and subgrain boundaries may break away from pining of these fine particles, which makes contribution to the serrated flow stress−strain curves (Fig. 2). At the lowest Z value, i.e., ln Z=24.01, some small recrystallized grains can be found, and typical TEM image is given in Fig. 4(e); it is likely a recrystallized grain, which exhibits an equiaxed shape and is surrounded by HABs. Moreover, the bulging of HAB was also observed under this condition (Fig. 4(f)). It seems that there is a low density of Al_3Zr dispersoids in this region, which cannot retard migration of this HAB, and thus the recrystallized grain can grow into the adjacent grains with many dislocations. This result may support the SIBM mechanism of DRX during hot compression.

Apart from hot deformation parameters such as high temperature and low strain rate for SIBM to occur, another factor may be the initial inhomogeneous microstructure, which gives rise to nonuniform distribution of dislocations and subgrains (Fig. 2). The presence of grain boundaries is partly responsible for the different deformation performances of grains under the same deformation condition. Another reason may be the nonuniform distribution of the recrystallization inhibitor Al_3Zr dispersoids. In general, there is an inhomogeneous distribution of Zr in Al−Zn−Mg−Cu−Zr alloys due to peritectic reaction during solidification [24]. Zr element tends to be enriched at the center of grains but depleted in the regions close to grain boundaries. Figure 5 gives EPMA images and line scanning results of Zr element. The shape of grains is visible as the GBs are decorated

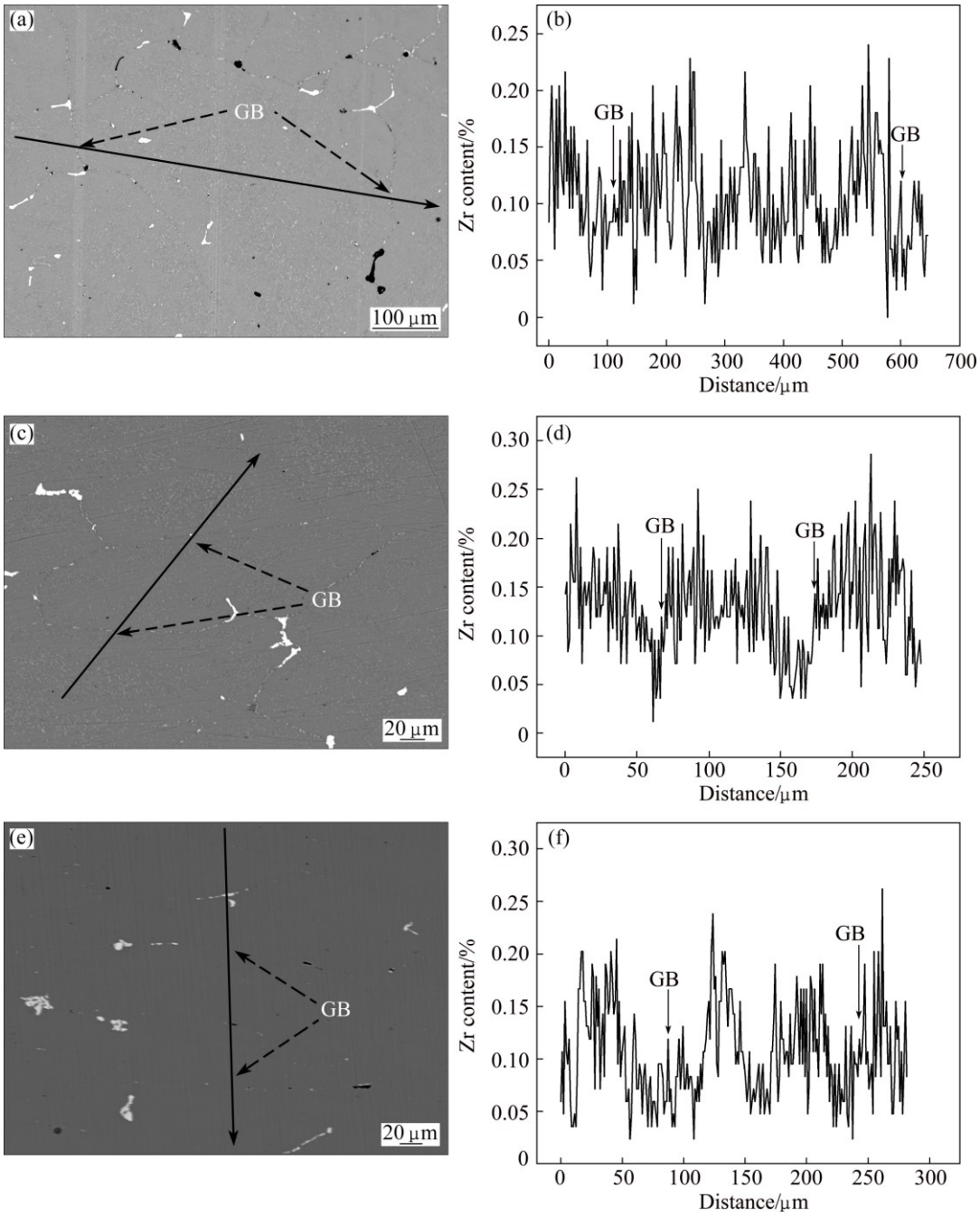

Fig. 5 EPMA images and line scanning results of Zr element in various specimens: (a, b) Homogenizated; (c, d) ln Z=36.10 (623 K, 10 s^{-1}); (e, f) ln Z=24.01 (723 K, 0.01 s^{-1})

by bright second phase particles. From Figs. 5(b)−(f), in both the homogenized and as-deformed specimens, the content of Zr is lower near GBs than in the central regions of the grain. As a result, there is a higher density of Al_3Zr dispersoids in the interior of grains, which may make this region harder than those close to GBs. Therefore, a large gradient of dislocations is likely to appear. Simultaneously, the lack of Al_3Zr dispersoids adjacent to the initial GBs is favorable for bulging of GBs. These factors can make contribution to SIBM during hot compression at low Z values.

4 Conclusions

1) At high Z values, the softening mechanism of 7085 aluminum alloy is dominated by dynamic recovery during hot compression. With the decrease of Z value, dynamic recrystallization tends to occur. The largest fraction of DRX about 10.2% is obtained under the hot compression condition with ln Z=24.01 (723 K, 0.01 s^{-1}).

2) Strain-induced boundary migration is the likely dynamic recrystallization mechanism during hot

compression with ln Z=24.01 (723 K, 0.01 s^{-1}). The inhomogeneous distribution of Al_3Zr dispersoids can make contribution to strain-induced boundary migration.

References

[1] MCQUEEN H J. Development of dynamic recrystallization theory [J]. Materials Science and Engineering A, 2004, 387−389: 203−208.

[2] QUAN G Z, LIU K W, ZHOU J, CHEN B. Dynamic softening behaviors of 7075 aluminum alloy [J]. Transactions of Nonferrous Metals Society of China, 2009, 19(S3): s537−s541.

[3] GOURDET S, MONTHEILLET F. Effects of dynamic grain boundary migration during the hot compression of high stacking fault energy metals [J]. Acta Materialia, 2002, 50: 2801−2812.

[4] ROKNI M R, ZAREI-HANZAKI A, ROOSTAEI A A. An investigation into the hot deformation characteristics of 7075 aluminum alloy [J]. Materials and Design, 2011, 32: 2339−2344.

[5] SHI C J, LAI J, CHEN X G. Microstructural evolution and dynamic softening mechanisms of Al−Zn−Mg−Cu alloy during hot compressive deformation [J]. Materials Science and Engineering A, 2014, 7: 244−264.

[6] TSIVOULAS D, PRANGNELL P B. The effect of Mn and Zr dispersoid-forming additions on recrystallization resistance in Al−Cu−Li AA2198 sheet [J]. Acta Materialia, 2014, 77: 1−16.

[7] LIN Y J, LIU W C, WANG L M. Ultra-fine grained structure in Al−Mg induced by discontinuous dynamic recrystallization under moderate straining [J]. Materials Science and Engineering A, 2013, 573: 197−204.

[8] KAIBYSHEV R, SITDIKOV O, GOLOBORODKO A. Grain refinement in as-cast 7475 aluminum alloy under hot deformation [J]. Materials Science and Engineering A, 2003, 344: 348−356.

[9] ASHTIANI H R R, PARSA M H, BISADI H. Effects of initial grain size on hot deformation behavior of commercial pure aluminum [J]. Materials and Design, 2012, 42: 478−485.

[10] HUMPHREYS F J, HATHERLY M. Recrystallization and related annealing phenomena [M]. 2nd ed. Amsterdam: Elsevier, 2004.

[11] YANG X Y, MIURA H, SAKAI T. Continuous dynamic recrystallization in a superplastic 7075 aluminum alloy [J]. Materials Transaction, 2002, 43(10): 2400−2407.

[12] WILLIAMS J C, EDGAR A S J. Progress in structural materials for aerospace systems [J]. Acta Materialia 2003; 59: 5775−5799.

[13] HAN N M, ZHANG X M, LIU S D. Effects of solution treatment on the strength and fracture toughness of aluminum alloy 7050 [J]. Journal of Alloys and Compounds, 2011, 509(10): 4138−4145.

[14] KANNAN M B, RAJA V S. Enhancing stress corrosion cracking resistance in Al−Zn−Mg−Cu−Zr alloy through inhibiting recrystallization [J]. Engineering Fracture Mechanics, 2010, 77: 249−256.

[15] LIU S, LIU W, ZHANG Y, ZHANG X, DENG Y. Effect of microstructure on the quench sensitivity of AlZnMgCu alloys [J]. Journal of Alloys and Compounds, 2010, 507: 53−61.

[16] LÜ X Y, GUO E J, ROMETSCH P. Effect of one-step and two-step homogenization treatments of distribution of Al_3Zr dispersoids in commercial AA7150 aluminium alloy [J]. Transactions of Nonferrous Metals Society of China, 2012, 22: 2645−2651.

[17] ZHENG Y, LI C, LIU S, DENG Y, ZHANG X. Effect of homogenization time on quench sensitivity of 7085 aluminum alloy [J]. Transactions of Nonferrous Metals Society of China, 2014, 24: 2275−2281.

[18] LIU S D, YUAN Y B. LI C B, YOU J H, ZHANG X M. Influence of cooling rate after homogenization on microstructure and mechanical properties of aluminum alloy 7050 [J]. Metals and Materials International, 2012, 18: 679−683.

[19] DENG Y L, WAN L, ZHANG Y, ZHANG X M. Evolution of microstructure and textures of 7050 Al alloy hot-rolled plate during staged solution heat-treatments [J]. Journal of Alloys and Compounds, 2010, 498: 88−94.

[20] ZHANG H, JIN N, CHEN J. Hot deformation behavior of Al−Zn−Mg−Cu−Zr aluminum alloys during compression at elevated temperature [J]. Transactions of Nonferrous Metals Society of China, 2011, 21: 437−442.

[21] LIU S, YOU J, ZHANG X, DENG Y, YUAN Y. Influence of cooling rate after homogenization on the flow behavior of aluminum alloy 7050 under hot compression [J]. Materials Science and Engineering A, 2010, 527: 1200−1205.

[22] MIRZADEH H, NAJAFIZADEH A. Prediction of the critical conditions for initiation of dynamic recrystallization [J]. Materials and Design, 2010, 31: 1174−1179.

[23] ZHANG D. Recrystallization control in hot deformation and its effects on quench sensitivity for aluminum alloy 7085 [D]. Changsha: Central South University, 2015. (in Chinese)

[24] DENG Y, ZHANG Y, WAN L, ZHU A A. ZHANG X. Three-stage homogenization of Al−Zn−Mg−Cu alloys containing trace Zr [J]. Metallurgical and Materials Transactions A, 2013, 44 : 2470−2477.

7085 铝合金的热变形动态再结晶行为

李东锋[1,2,3]，张端正[1,2]，刘胜胆[1,2,4]，单朝军[1,2]，张新明[1,2,4]，王 琴[1,2]，韩素琦[1,2]

1. 中南大学 材料科学与工程学院，长沙 410083；
2. 中南大学 有色金属材料科学与工程教育部重点实验室，长沙 410083；
3. 湖南工程学院 机械工程学院，湘潭 411104；
4. 中南大学 有色金属先进结构材料与制造协同创新中心，长沙 410083

摘 要：通过电子背散射衍射(EBSD)、电子探针(EPMA)和透射电子显微镜(TEM)研究 7085 铝合金在温度 573~723 K、变形速率 0.01~10 s^{-1} 条件热压缩时的动态再结晶行为。结果表明，在高 Zener−Hollomon (Z)值时，动态回复是主要的软化机制；随着 Z 参数值降低，出现动态再结晶。在 ln Z=24.01 (723 K，0.01 s^{-1})热压缩时，动态再结晶分数最高，为 10.2%。EBSD 结果表明，再结晶晶粒出现在初始晶界附近，其取向与变形晶粒接近。应变诱发晶界迁移是最可能的动态再结晶机制。晶界附近的低密度 Al_3Zr 弥散粒子有利于应变诱发晶界迁移的发生。

关键词：铝合金；Zener−Hollomon 参数；动态再结晶；应变诱发晶界迁移；Al_3Zr 弥散粒子

(Edited by Xiang-qun LI)